MODELING OF AN AUTONOMOUS MICROGRID FOR FREQUENCY STABILITY ANALYSIS

I. ŞERBAN[1] C. MARINESCU[1]

Abstract: *This paper presents a reduced-order model for an autonomous microgrid (MG) consisting in a micro hydro power plant (MHPP), a wind power plant (WPP) and a battery energy storage system (BESS). The model is developed for frequency stability analysis. The BESS controls the active power flow in the MG by using a properly tuned frequency controller. The model is developed with the purpose of frequency stability analysis of the MG. The results are focused on frequency response for variable load and variable wind speed.*

Key words: *microgrid, micro-hydro power plant, wind power plant, energy storage, frequency control.*

1. Introduction

Renewable energy sources (RES) have begun to have an important role in the developing of electrical power systems, representing a new step towards distributed generation. Hybrid power systems represent a combination of several RES operating as one entity. These systems are often grouped into single-phase and three-phase micro-grids (MG) and supply mostly domestic loads in remote areas. A typical MG contains several energy sources and consumers, producing electrical and sometimes thermal energy. Controlling such systems involves the use of interfacing, protective and control elements for each generator and devices to regulate the voltage and frequency.

The MG operates autonomously or can be interconnected with the national grid. In autonomous operating mode, the generating units should share the active and reactive power in the MG, and they have to maintain the stability of the system. The control problem of autonomous is a continuously studied issue [9], [12], [13], mainly regarding the frequency stability. In an autonomous MG with RES, predominating wind power, power balance is difficult to achieve, mainly because of the wind power variations, difficult to predict. An efficient way to overcome this problem is to use an energy storage system that acts as a buffer between generators and loads. The energy storage system can be implemented with various type of batteries [1], fuel cells [13], or combination of both [8].

Other solutions use dump loads [14], combination of energy storage and dump loads [15] or load shedding.

2. System Configuration

The studied system in this paper, presented in Figure 1, consists in a micro-hydro

[1] Dept. of Electrical Engineering, *Transilvania* University of Braşov.

power plant (MHPP), a wind power plant (WPP) and a battery energy storage system (BESS).

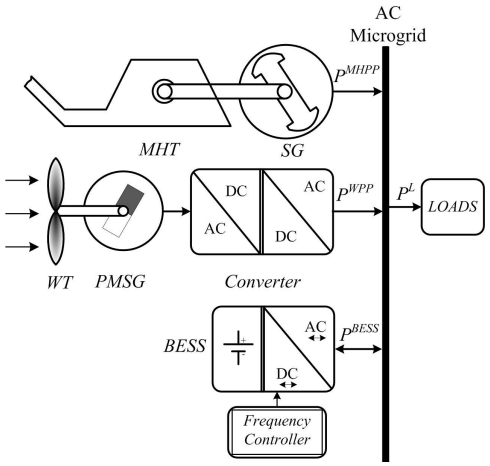

Fig. 1. *MG system configuration*

They are all connected on an AC single-phase MG that operates in autonomous mode. The MHPP is equipped with a synchronous generator (SG) driven by a Pelton micro-hydro turbine (MHT). The SG forms the MG voltage and controls the reactive power flow in the system through a voltage controller, placed on the SG field winding side. In the following, the voltage is considered kept constant to the rated value and its variations with the load are neglected. This approximation is fair because the voltage control loop has much smaller time constants (approximately ten times as a rule of thumb) than those involved in the frequency control. The dominant time constant in the frequency control loop is the MHT inertia, as will be presented in the following.

The WPP is a variable-speed scheme with a multi-pole permanent magnet synchronous generator (PMSG) directly connected to the wind turbine (WT). A converter, consisting in a three-phase diode rectifier and a single-phase inverter, accomplishes the interface between the generator and MG. The inverter injects active power at unity power factor, without any frequency or voltage control at the point of common coupling.

The BESS ensures the active power balance in the MG, acting as a load or as a generator according to the generation and demand. The BESS internal structure can take several forms, but this paper does not study this aspect. A standard lead-acid battery is considered for energy storage. Neglecting the power losses in the system, the active power balance is:

$$P^{BESS} = P^{MHPP} + P^{WPP} - P^{L}, \qquad (1)$$

where: P^{BESS} is the BESS power (positive or negative); P^{MHPP} is the MHPP active power; P^{WPP} is the WPP active power and P^{L} is the loads power.

To maintain the system's frequency within required limits (±1% in steady-state) the active power balance must be ensured in any moment. The main sources of disturbances are the WPP, which injects variable active power according to the wind speed, and the loads that varies quasi-randomly.

In transitory regime, the MG frequency varies, according to the active power imbalance and the frequency controller has to restore it by adding more power in the system.

The literature presents various schemes for controlling the frequency and they are divided mainly in two solutions. The first solution is based on measuring the power and control the output frequency [4], [5], while the second one consists in measuring the system frequency and control the active power [6], [14], [16]. The last solution is adopted in this paper too.

In this case, the frequency controller maintains the active power balance by controlling the BESS power flow. Of course, this is done with some limitations given by the storage capabilities and the

BESS rated power.

A proper frequency response depends of the frequency controller tuning and this is another aspect that is studied in this paper.

3. MG Modelling

3.1. MHPP Model

The MHT does not include a speed-governor, and it operates at full power, in an optimum efficiency point. The SG injects the active power into the MG and performs the voltage control by modifying the reactive power flow.

In most of the cases, the dynamics of the power unit can be expressed by using only the inertia moment of the unit [18], which is much larger than other time constants involved in the system. The SG and MHT are connected through a rigid shaft, and their inertia moment has a predominant impact over the system's transitory response. The SG is directly connected to the MG and it will be modelled only as an amplifier, neglecting the electrical time constants. The MG frequency is directly proportional with the SG rotor speed. Thereby, the MHT is rigidly connected to the MG and this feature is a very important advantage of this configuration because the MHT lends more stability to the MG and more strength.

The SG and MHT assembly is characterized by the equation of motion in per unit (p.u.):

$$T_m^{MHT} - T_e^{SG} = 2H^{MHT} \cdot \frac{\mathrm{d}\omega_r^{MHT}}{\mathrm{d}t} + K_D^{MHT} \omega_r^{MHT}, \tag{2}$$

where: T_m^{MHT} is the MHT mechanical torque; T_e^{SG} is the electromagnetic torque of the SG (neglecting the system's losses); H^{MHT} is the combined inertia time constant of the turbine and generator [s]; ω_r^{MHT} is the angular velocity of the common shaft [rad/s]; K_D^{MHT} is the damping factor of the MHT (self-regulation).

For small deviations it may be used power instead of torques [3], in p.u.:

$$\Delta P_m^{MHT} - \Delta P_e^{SG} = 2H^{MHT} \cdot \frac{\mathrm{d}\Delta\omega_r^{MHT}}{\mathrm{d}t} + K_D^{MHT} \Delta\omega_r^{MHT}. \tag{3}$$

The value of K_D^{MHT} in the nominal operating point is equal to the partial derivative of the mechanical power with the speed:

$$K_D^{MHT} = -\left.\frac{\partial P_m^{MHT}}{\partial \omega_r^{MHT}}\right|_{\omega_r^{MHT}=1\,[p.u.]}. \tag{4}$$

Because the turbine flow is considered constant, the mechanical power of the MHT is constant and $\Delta P_m^{MHT} = 0$. Thereby, we are interested of the MHPP response only when the load changes, so the transfer function of speed/MHPP output power is expressed as:

$$G^{MHPP}(s) = \frac{\Delta\omega_r^{MHT}}{\Delta P^{MHPP}} = \frac{-1}{2H^{MHT} \cdot s + K_D^{MHT}}. \tag{5}$$

The MG frequency deviation is equal to (in p.u.) $\Delta f = \Delta\omega_r^{MHT}$.

3.2. WPP Model

Aerodynamic model

The amount of mechanical power captured from wind by a three-blade wind turbine can be expressed as [17]:

$$P_m^{WT} = \frac{\rho}{2} c_p(\lambda,\beta)\, A\, v_w^3, \tag{6}$$

where: ρ is the mass density of air [kg/m^3]; A is the blades' swept area [m^2]; v_w is the velocity of the wind [m/s]; $c_p(\lambda, \beta)$ is the power coefficient of the wind turbine; λ is tip speed ratio of the rotor blade tip speed to wind speed; β is the blades pitch angle [deg].

The wind turbine considered is passive stall controlled, so $\beta = 0$ and the tower shadow and wind shear effects are neglected.

The WPP is interfaced with the MG by a current controlled PWM inverter, which injects power at unity power factor. The mainly used control strategies for grid-connected inverters are presented in [2]. The inverter response is very fast relative to the other time constants in the WPP dynamics and therefore it will be modelled as a simple amplifier.

The injected power into the grid depends linear of the DC bus, being defined a minimum and a maximum DC voltage, corresponding to zero and rated power of the inverter. The characteristic of the DC bus voltage function of the WTG rotor speed can be approximated by a linear function estimated from experimental measurements. Therefore, the following relation expresses the relationship between the WPP power and WT rotor speed in the linear region, in per unit:

$$P^{WPP}(\omega_r^{WT}) = \frac{\omega_r^{WT} - \omega_{\min}}{1 - \omega_{\min}}, \qquad \omega_r^{WT} \in [\omega_{\min} ... 1], \tag{7}$$

where: $\omega_{\min}$ is the minimum rotor speed when the WPP begin to produce power.

Figure 2 shows the wind turbine characteristics function of rotor speed for different wind speeds, and the steady-state operating curve based on (7). Figure 3 shows the characteristic curve of the WPP output power versus wind speed, which will be used hereinafter for the WPP model. It results from (6) and (7).

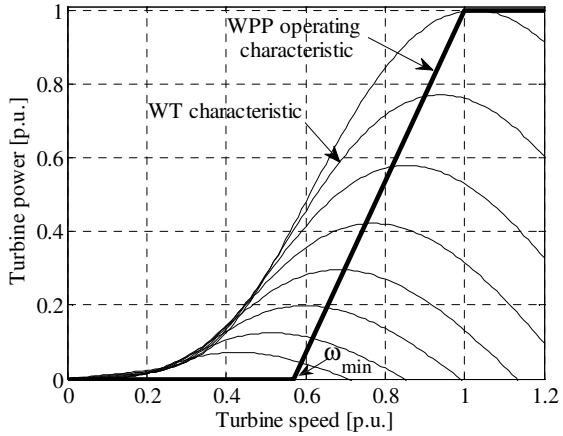

Fig. 2. *Wind Turbine characteristics and steady-state operating curve*

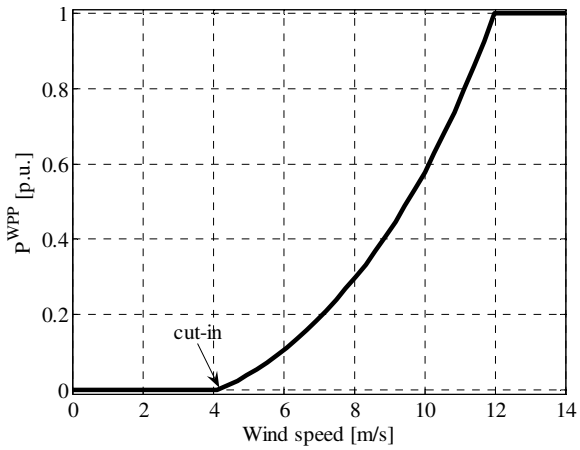

Fig. 3. *WPP output power vs. wind speed*

Small-signal wind turbine model

The wind turbine is a nonlinear element in the WPP model and its characteristics depends of the wind speed and rotor speed. For small-signal modelling purpose the characteristic can be linearised in different steady-state operating points, by using the following expression:

$$\Delta P_m^{WPP} = K_\omega^{WT} \cdot \Delta\omega_r^{WT} + K_w^{WT} \cdot \Delta v_w , \quad (8)$$

where: K_ω^{WT} and K_w^{WT} are the partial derivatives of the mechanical power, as follows:

$$K_\omega^{WT} = \left.\frac{\partial P_m^{WT}}{\partial \omega_r^{WT}}\right|_{v_w = ct},$$

and

$$K_w^{WT} = \left.\frac{\partial P_m^{WT}}{\partial v_w}\right|_{\omega_r = ct}. \quad (9)$$

The dynamics of the WPP involves mechanical and electrical time constants. The wind turbine is directly connected with the PMSG by a rigid shaft and therefore a one-mass equivalent model of the mechanical drive train will be considered. The model is described by the following equation of motion in per unit, where for small deviations it may be used power instead of torques [3]:

$$\Delta P_m^{WT} - \Delta P_e^{PMSG} = 2H^{WT} \frac{\mathrm{d}\Delta\omega_r^{WT}}{\mathrm{d}t}, \quad (10)$$

where: P_m^{WT} is the mechanical power; P_e^{PMSG} is the electrical power of the PMSG - neglecting system's losses; ω_r^{WT} is the angular velocity of the common shaft; H^{WT} is the combined inertia constant of the wind turbine and generator.

The speed/mechanical power transfer function is expressed as:

$$G_m^{WPP}(s) = \frac{\Delta\omega_r^{WT}}{\Delta P_m^{WT}} = \frac{1}{2H^{WT} \cdot s}. \quad (11)$$

The dynamic behaviour of the PMSG - electrical converter power path is considered a first order lag, as given next:

$$G_e^{WPP}(s) = \frac{\Delta P_e^{PMSG}}{\Delta\omega_r^{WT}} = \frac{K_e}{1 + \tau_e \cdot s}, \quad (12)$$

where: K_e is the amplification factor in per unit and depends of the wind turbine rated power; τ_e is the time delay between the wind turbine speed change and the electrical power injected into the grid by the inverter.

The first order filter acts as a decoupling element between the wind turbine and the grid-side inverter.

The electronically interfaced generators are much faster than conventional rotating machines and they do not have the capability of storing energy during transients [11]. While in a conventional rotating machine, the mechanical inertia of the rotor influences the frequency stability, in an electronically interfaced generator the main source of oscillations is the PLL (Phase Locked Loop) [7]. It ensures the synchronization of the inverter voltage with the grid voltage. Proper selection of its parameters ensures good system stability.

Because the studied system includes a large time constant, H^{MHT}, and the PLL time constant, is much smaller, the PLL influence over the system response is negligible.

Therefore, the WPP is modelled by the following transfer function:

$$G^{WPP}(s)=\frac{\Delta P^{WPP}}{\Delta v_w}=\frac{K_w^{WT}K_e}{2H^{WT}\tau_e\cdot s^2+(2H^{WPP}-K_\omega^{WT}\tau_e)\cdot s+K_e-K_\omega^{WT}}. \quad (13)$$

3.3. Frequency Controller Model

As has been presented in section 2, the active power balance in the MG is ensured by the BESS that acts as a load or as a generator.

A single-phase inverter interfaces the BESS DC-link with the MG. Same remarks as for the WPP inverter, presented in section 3.2., regarding the PLL influence over the system response, are valid. Thus, the BESS is modelled only by an amplifier. The frequency controller drives the BESS. The controller is a PI structure and it acts on the frequency deviation, increasing or decreasing the BESS power. The transfer function of the frequency/BESS active power reference in p.u. is:

$$G^{BESS}(s)=\frac{\Delta P^{BESS}}{\Delta f}=K_P+\frac{K_I}{s}. \quad (14)$$

The controller is discretized with a sample time of 20 ms.

In a practical implementation, the BESS power is limited at a certain level, and for our study, we will consider that the BESS rated power is less than the MG power.

The limitations given by the battery state-of-charge are not considered in this study.

3.4. Overall System Model

Based on Eq. (1)…(14), the block diagram of the entire system including MHPP, WPP and BESS with the frequency controller, is presented in Figure 4. The model has two inputs, one is the load power deviation (ΔP^L) and the other is the wind speed deviation (Δv_w). The loads are considered frequency independent and therefore they are modelled as constants. The function of the load frequency controller is to eliminate the mismatch created either by the small load power change or due to the variation of the wind power. The results we are interested of are the MG frequency deviation for various cases.

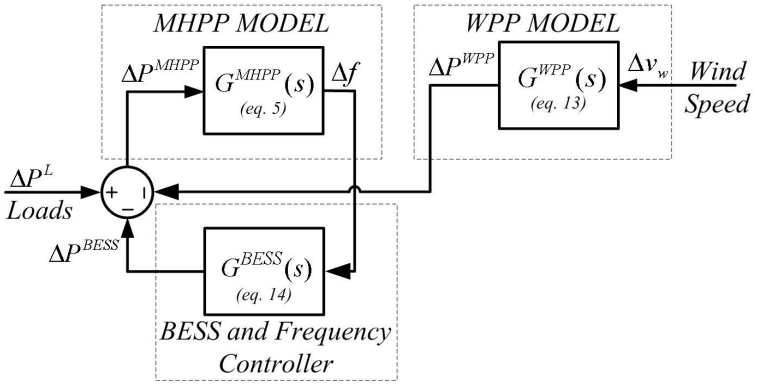

Fig. 4. *The MG block diagram*

The system can be modelled by the following expression:

$$\Delta f = G_1(s) \cdot \Delta P^L(s) + G_2(s) \cdot \Delta v_w(s) \,, \quad (15)$$

where:

$$G_1(s) = \frac{\Delta f}{\Delta P^L} = \\ = \frac{G^{MHPP}(s)}{1 + G^{MHPP}(s) \cdot G^{BESS}(s)}, \quad (16)$$

$$G_2(s) = \frac{\Delta f}{\Delta v_w} = \\ = \frac{G^{MHPP}(s) G^{WPP}(s)}{1 + G^{MHPP}(s) \cdot G^{BESS}(s)}. \quad (17)$$

It can be observed that in the transfer function $G_1(s)$ the WPP transfer function is not present because, as been stated previously, the WPP output power does not depends of the MG frequency.

4. Results and Discussion

The components of the MG have the following rated powers: $P^{MHPP} = 5$ kW, $P^{WPP} = 3$ kW and $P^{BESS} = 5$ kW. The base power for unitization is $P_{base} = 5$ kW.

4.1. Tuning the Frequency Controller

Based on the small-signal system modelling presented in section 3, the frequency controller is tuned for optimal frequency response. Several methods can be used to achieve this goal [10].

The optimal parameters of the PI controller (K_p and K_i) are presented in Table 1, along with the settling time T_{set} and the maximum frequency deviation, $\Delta f_{\max}$ for 10% load step. Figure 5 presents the two-pairs of complex-conjugate dominant poles when K_p varies from 0 to 30. For K_p = 22 the oscillation frequency of the poles is 0.83 Hz and the damping factor is around 0.74. A bigger amplification factor will lead to a higher damping but its effect upon the noise and measurement errors has to be taken into account also. The optimal value of K_p has to be adjusted in the practical implementation stage.

Controller parameters Table 1

K_p	K_i	T_{set},[s]	$\Delta f_{\max}$, [p.u.]
22	75.5	0.82	0.0031

Figure 6 presents the frequency deviation (Δf) and the frequency controller response or the BESS power (ΔP^{BESS}) for a 10% load power step. After a short transitory regime

(less than one second), the frequency deviation returns to zero and the BESS power will stabilize at –0.1 p.u., ensuring the active power balance in the MG.

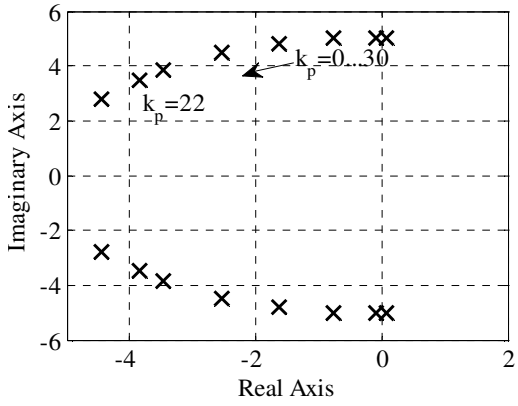

Fig. 5. *Trace of dominant poles for K_p = 0…30*

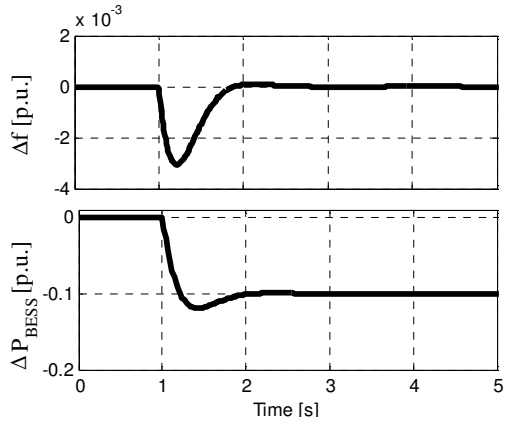

Fig. 6. *Frequency deviation* (Δf) *and BESS power* (ΔP^{BESS}) *for 10% load step*

Another aspect that can be studied with the proposed model is the influence of the wind speed variations over the frequency stability. Figure 7 presents the frequency deviation (Δf) and the frequency controller response or the BESS power (ΔP^{BESS}) for 1% wind speed increase at different wind speeds (5, 8, and 12 m/s). Because the wind turbine mechanical characteristic is nonlinear (presented in section 3.2), the slopes from (9) varies according to the wind speed. Therefore, the effect of the wind speed change over the MG frequency is different depending of the absolute wind speed value.

As presented in section 3.2., the WPP inverter active power is considered frequency independent. The assumption is fair because the MHPP inertia time is much larger than the WPP response. Therefore, the WPP operating point has a minor impact over the system's stability.

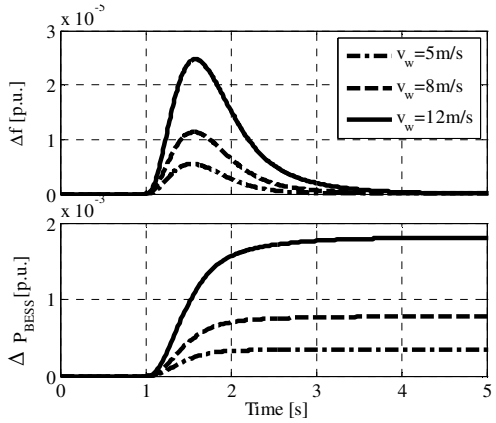

Fig. 7. *Frequency deviation* (Δf) *and BESS power* (ΔP^{BESS}) *for 1% wind speed change*

5. Conclusions

The paper has presented a method for modelling an autonomous microgrid (MG) for frequency stability analysis. The MG consists in a micro-hydro power plant (MHPP), a wind power plant (WPP) and a battery energy storage system (BESS), which has the role of maintaining the active power balance in the system.

The model took into account only the dominant elements of the system, which are involved in the MG frequency control, thus reducing the complexity of the model.

The tuning of the frequency controller is an important step in the MG developing process, and the presented model can be very useful in this regard.

The results were focused on load power and wind speed variations and the frequency response was shown.

Acknowledgment

This research theme is under the project CNCSIS IDEI 134/2007, supported by The Romanian Ministry of Education Research and Innovation.

References

1. Barote, L., Weissbach, R., et al.: *Stand-Alone Wind System with Vanadium Redox Battery Energy Storage*. In: Proceedings of OPTIM'08, vol II-B, May 2008, Braşov, Romania, p. 407-412.
2. Blaabjerg, F., Teodorescu, R., et al.: *Overview of Control and Grid Synchronization for Distributed Power Generation Systems*. In: IEEE Trans. Industrial Electronics **53** (2006) No. 5, p. 1398-1409.
3. Boldea, I.: *Synchronous Generators - The Electric Generators Handbook.* CRC Press, USA, 2006.
4. Engler, A., Hardt, C., et al.: *Parallel Operation of Generators for Stand-Alone Single-Phase Hybrid Systems.* In: EPVSEC, October 2001, Munich, p. 1-4.
5. Guerrero, J.M., Matas, J., et al.: *Wireless-Control Strategy for Parallel Operation of Distributed-Generation Inverters*. In: IEEE Trans. Industrial Electronics **53** (2006) No. 5, p. 1461-1470.
6. Katiraei, F., Iravani, M.R., Lehn, P.W.: *Small-Signal Dynamic Model of a*

Micro-Grid Including Conventional and Electronically Interfaced Distributed Resources. In: IET Generation, Transmission & Distribution **1** (2007) No. 3, p. 369-378.
7. Katiraei, F., Iravani, M.R.: *Power Management Strategies for a Microgrid with Multiple Distributed Generation Units*. In: IEEE Trans. Power Systems **21** (2006) No. 4, p. 1821-1831.
8. Lee, D.J., Wang, L.: *Small-Signal Stability Analysis of an Autonomous Hybrid Renewable Energy Power Generation/Energy Storage System Part I: Time-Domain Simulations.* In: IEEE Trans. Energy Conv. **23** (2008) No. 1, p. 311-320.
9. Lopes, J.A., Moreira, C.L., Madureira, A.G.: *Defining Control Strategies for MicroGrids Islanded Operation.* In: Trans. Power Systems **21** (2006) No. 2, p. 916-924.
10. O'Dwyer, A.: *Handbook of PI and PID Controller Tuning Rules.* London. Imperial College Press, 2003.
11. Piagi, P., Lasseter, R.H.: *Autonomous Control of Microgrids*. In: IEEE PES Meeting, Montreal, June 2006, p. 1-8.
12. Piagi, P.: *Microgrid Control*. In: Ph.D. Thesis, University of Wisconsin-Madison, 2005.
13. Senjyu, T., Nakaji, T., et al.: *A Hybrid Power System Using Alternative Energy Facilities in Isolated Island.* In: IEEE Trans. Energy Conversion **20** (2005) No. 2, p. 406-414.
14. Şerban, I., Ion, C.P., Marinescu, C.: *Frequency Control and Unbalances Compensation in Stand-Alone Fixed-Speed Wind Turbine Systems.* In: Proceedings of IECON'08, Florida, USA, 2008, p. 2167-2172.
15. Şerban, I., Marinescu, C.: *A Solution for Frequency Control in Islanded Three-Phase Micro-Grids Supplied by Renewable Energy Sources.* In: Proceedings of OPTIM'08, Braşov, Romania, 2008, p. 327-332.
16. Şerban, I., Marinescu, C.: *Power Quality Issues in a Stand-Alone Microgrid Based on Renewable Energy*. In: Revue Roumaine des Sciences Techniques. Électrotechn. et Énerg. **53** (2008) No. 3, p. 285-293.
17. Siegfried, H.: *Grid Integration of Wind Energy Conversion Systems.* Second Edition, John Wiley & Sons Ltd, USA, 2006.
18. Strah, B., Kuljaca, O., Vukic, Z.: *Speed and Active Power Control of Hydro Turbine Unit*. In: IEEE Trans. Energy Conv. **20** (2005) No. 2, p. 424-434.